Chemosphere 324 (2023) 138348

Contents lists available at ScienceDirect

Chemosphere

journal homepage: www.elsevier.com/locate/chemosphere

Early-life exposure to environmentally relevant concentrations of triclocarban impairs ocular development in zebrafish larvae

Giulia Caioni [a,1], Carmine Merola [b,1], Cristiano Bertolucci [c], Tyrone Lucon-Xiccato [c], Beste Başak Savaşçı [b,d], Mara Massimi [a], Martina Colasante [a], Giulia Fioravanti [e], Nunzio Antonio Cacciola [f], Rodolfo Ippoliti [a], Michele d'Angelo [a], Monia Perugini [b,*], Elisabetta Benedetti [a]

[a] Department of Life, Health and Environmental Sciences, University of L'Aquila, L'Aquila, Italy
[b] Department of Bioscience and Agro-Food and Environmental Technology, University of Teramo, Teramo, Italy
[c] Department of Life Sciences and Biotechnology, University of Ferrara, Ferrara, Italy
[d] Unit of Evolutionary Biology/Systematic Zoology, Institute for Biochemistry and Biology, University of Potsdam, Potsdam, Germany
[e] Department of Physical and Chemical Sciences University of L'Aquila, L'Aquila, Italy
[f] Department of Veterinary Medicine and Animal Production, University of Naples Federico II, Naples, Italy

HIGHLIGHTS

- TCC induces microphthalmia in zebrafish larvae at environmentally relevant concentrations.
- Microphthalmia is accompanied with alterations in retinal structure.
- Molecular analysis revealed a change in the transcript abundance of genes required in eye development.
- Early life exposure to TCC has long-term effects, acting on visual discrimination abilities.

GRAPHICAL ABSTRACT

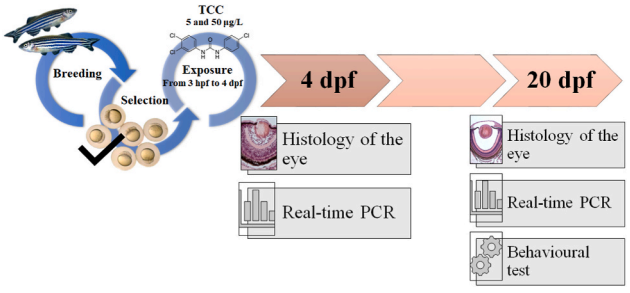

ARTICLE INFO

Handling Editor: James Lazorchak

Keywords:
Triclocarban
Zebrafish
Ocular developmental toxicity
Eyesight
Retina

ABSTRACT

Triclocarban (TCC), is an antimicrobial component in personal care products and it is one of the emerging contaminants since it has been detected in various environmental matrices. Its presence in human cord blood, breast milk, and maternal urine raised issues about its possible impact on development and increased concerns about the safety of daily exposure.

This study aims to provide additional information about the effects of zebrafish early-life exposure to TCC on eye development and visual function. Zebrafish embryos were exposed to two concentrations of TCC (5 and 50 µg/L) for 4 days. TCC-mediated toxicity was assessed in larvae at the end of exposure and in the long term (20 days post fertilization; dpf), through different biological end-points. The experiments showed that TCC exposure

* Corresponding author. ;
E-mail addresses: giulia.caioni@guest.univaq.it (G. Caioni), cmerola@unite.it (C. Merola), cristiano.bertolucci@unife.it (C. Bertolucci), tyrone.luconxiccato@unife.i (T. Lucon-Xiccato), basak.savasci@uni-potsdam.de (B.B. Savaşçı), mara.massimi@univaq.it (M. Massimi), martina.colasante@guest.univaq.it (M. Colasante), giulia.fioravanti@univaq.it (G. Fioravanti), nunzioantonio.cacciola@unina.it (N.A. Cacciola), rodolfo.ippoliti@univaq.it (R. Ippoliti), michele.dangelo@univaq.it (M. d'Angelo), mperugini@unite.it (M. Perugini), elisabetta.benedetti@univaq.it (E. Benedetti).
[1] These authors contributed equally.

https://doi.org/10.1016/j.chemosphere.2023.138348
Received 27 December 2022; Received in revised form 6 March 2023; Accepted 7 March 2023
Available online 8 March 2023

Behavior
Visual discrimination abilities

influences the retinal architecture. In 4 dpf treated larvae, we found a less organized ciliary marginal zone, a decrease in the inner nuclear and inner plexiform layers, and a decrease in the retinal ganglion cell layer. Photoreceptor and inner plexiform layers showed an increase in 20 dpf larvae at lower and both concentrations, respectively. The expression levels of two genes involved in eye development (*mitfb* and *pax6a*) were both decreased at the concentration of 5 μg/L in 4 dpf larvae, and an increase in *mitfb* was observed in 5 μg/L-exposed 20 dpf larvae. Interestingly, 20 dpf larvae failed to discriminate between visual stimuli, demonstrating notable visual perception impairments due to compound. The results prompt us to hypothesize that early-life exposure to TCC may have severe and potentially long-term effect on zebrafish visual function.

1. Introduction

Antimicrobial preservatives are added to cosmetics and personal care products to inhibit the development of microorganisms, ensuring the consumer product safety (Halla et al., 2018). Triclocarban (TCC) is an active ingredient in many skin-care products, including soap bars, cleansing lotions and antibacterial wipes (Schebb et al., 2011; Iacopetta et al., 2021). It ranked in the top ten contaminants of emerging concern (CEC), because of its diffusion on the surface waters and in the aquatic sediment phase (Halden and Paull, 2005; Chalew and Halden, 2009), and its tendency to accumulate in aquatic organisms (Coogan et al., 2007; Prosser et al., 2014; Das Sarkar et al., 2020). As a result of the frequent exposure, TCC has been also detected in human samples, such as blood (Wei et al., 2017), urine (Pycke et al., 2014), breast milk (Azzouz et al., 2016), and nails (Shi et al., 2013). Many studies showed an estrogenic disruption activity of TCC (Cao et al., 2020; Ahn et al., 2008; Huang et al., 2014; Zenobio et al., 2014), and its ability to influence thyroid hormone homeostasis (Hinther et al., 2011; Wu et al., 2016a).

In our previous study (Caioni et al., 2021), we demonstrated that environmentally relevant concentrations of TCC affected morphological traits and melanogenesis in zebrafish larvae. We found a strong microphthalmia in zebrafish larvae exposed to two concentrations of TCC (5 and 50 μg/L), even if the effects of this chemical on visual function and behavior remained unexplored. Chen et al. (2021) confirmed the significant reduction in eye size and the presence of altered retinal structures in larvae exposed to TCC from to 2–144 h post-fertilization (hpf), and also demonstrated changes in sensitivity to red and green light (Chen et al., 2021).

It remains unclear whether TCC alters the expression of eye development genes and affects behaviors driven by visual cues in larval fish. Moreover, assessing long-term effects deriving from larval exposure will be useful in evaluating TCC developmental toxicity. The present study was designed to understand the effects of TCC on zebrafish retina morphology and on vision function up to the late stage of larval development. For this purpose, we exposed zebrafish embryos from 3 hpf to two sublethal concentrations of TCC: 5 μg/L, an environmentally relevant concentration (Gomes et al., 2021), and 50 μg/L, the NOEC (No Observed Effect Concentration) value. Subjects at 4 and 20 dpf were collected to perform histological evaluations of the eyes, molecular analysis by Real-Time PCR and behavioral test to assess vision capabilities.

2. Materials and methods

2.1. Chemicals

TCC (CAS number 101−20–2, Pharmaceutical Secondary Standard; Certified Reference Material) was purchased from Merck Life Science, Milano, Italy. Dimethyl sulfoxide (DMSO) (>99.9% purity), 3,4-dichloroaniline (>98% purity), dichloromethane for analysis EMSURE® ACS, ISO, Reag. Ph Eur (>99.8%) and ethylenediaminetetraacetic acid tetrasodium salt (EDTA) were obtained from Merck Life Science (Co. St. Louis, MO, USA). Dilution water was prepared according to OECD TG 203, Annex 2 (OECD, 1992). Phosphate buffered saline (PBS) 1X was obtained from Corning (Mediatech, Inc., Manassas, VA, USA).

Formalin 37% and ethanol absolute were obtained from Sigma-Aldrich (Milano, Italy). Bio Clear was obtained from Bio Optica Milano, Italy. Paraffin pastilles (solidification point about 56–58 °C) were purchased from Merck, Life Science, Milano, Italy. Haematoxylin and eosin 1% aqueous solution was obtained from Merck Life Science, Milano, Italy. Eukitt® mounting medium was purchased from Bio Optica, Milano, Italy.

2.2. Zebrafish exposure to TCC

AB adults wild-type zebrafish were obtained from the breeding facility at the University of Teramo. Fish maintenance, breeding conditions, and egg production were described in detail in previous studies (Merola et al., 2020a, 2020b), and are in accordance with internationally accepted standards. At 2–3 hpf, embryos were examined under a dissecting microscope, and all healthy embryos at the blastula stage were randomly allocated to one of three experimental treatments. The treatments consisted of an environmentally relevant concentration of TCC (5 μg/L) and the NOEC value (50 μg/L) found in a previous study (Caioni et al., 2021), and a solvent control condition (DMSO, which was used to dissolve the TCC, at the final concentration of 0.01%). Each larva was treated individually in a 2 mL well; consequently, the number of replicates corresponds to the number of subjects per each treatment, which is reported below in the description of each specific assay performed. For Real-Time PCR at 4 dpf, 50 larvae for each condition were treated collectively in a beaker with 100 mL of dilution water. The treatment lasted until the larvae reached the age of 4 dpf, before they start to feed autonomously. At the end of exposure, a group of 4 dpf zebrafish larvae was euthanized and used for the histological analysis and Real-Time PCR (Table 1). The remaining zebrafish were maintained until the age of 20 dpf in glass tanks containing clean water (pH: 7 ± 0.2, conductivity: 500 ± 100 μS/cm, and dissolved O_2: 6.1 mg/L) in the incubator (temperature: 26 ± 1 °C, and photoperiod: 14 h light: 10 dark) and were fed with cultured live paramecia and dry feed (Zebrafeed, Sparos, Olhão, Portugal) three times per day. These remaining zebrafish larvae were used to perform histological analysis, Real-Time PCR and

Table 1
Number of zebrafish embryos used in the different investigations, and replicate number.

Real-Time PCR (4 dpf)	For each groups N = 50 for 3 biological replicates	50 larvae for each condition were treated collectively in a beaker with 100 mL of dilution water
Real-Time PCR (20 dpf)	For each groups N = 6 for 3 biological replicates	Each larva was treated individually in a well with 2 mL of dilution water
Histological analysis (4 dpf)	For each groups N = 10	Each larva was treated individually in a well with 2 mL of dilution water
Histological analysis (20 dpf)	For each groups N = 10	Each larva was treated individually in a well with 2 mL of dilution water
Visual discrimination (20 dpf)	TCC 5 μg/L N = 22; TCC 50 μg/L N = 17; solvent control N = 25.	Each larva was treated individually in a well with 2 mL of dilution water

the visual discrimination test at 20 dpf to evaluate the potential long-term effects of TCC early-life exposure (Table 1). Euthanasia of the larvae was performed with an overdose of Tricaine pharmaq (PHARMAQ AS, Norway). The work was carried out following the Italian law for protection of research animals D.L. n. 26 March 4, 2014 and the European regulation directive 2010/63/U: treatments were performed in non-feeding embryos; behavioral tests were simple observations of spontaneous swimming behavior designed to do not cause distress or harms in the subjects and their protocols were approved by Ethical Committee of University of Ferrara (OPBA TLX-2022-1).

2.3. Determination of TCC in exposure solution

The solutions were collected at 4 dpf. A control experiment was also conducted without embryos to assess the concentration of TCC in dilution water. Accordingly to Chen and collaborators (Chen et al., 2021), TCC concentrations in the exposure solution were analyzed by high-performance liquid chromatography (HPLC) combined with liquid-liquid extraction (LLE). For each condition 100 mL of exposure solution was combined with 20 mL of dichloromethane, shaking vigorously and extracting the organic phase. The extraction steps were repeated several times. All extracts were combined, and the dichloromethane was transferred into a 100 mL bottom flask and dried by a rotary evaporator (Strike 300, water bath temperature of 50 °C). The resultant residue was redissolved with 100 μL of methanol and analyzed by high-performance liquid chromatography (HPLC) using a C18 column (4.6 × 150 Luna, Phenomenex, Castel Maggiore, BO) and an analytical Azura HPLC apparatus (Knauer, Berlin, Germany) equipped with UV/Vis detector. Mobile phase ratio was methanol: water 80:20. The software used was Clarity7,4 by Data Apex Samples were run under isocratic conditions at 30 °C on C18 column. The injection volume was 100 μl and the flow rate was 1 mL/min.

TCC was identified on the basis of retention time (r.t. 5.7 min) at the optimized wavelength selected (258 nm). Each sample was run in triplicate. A robust calibration curve was built by using an external standard method, with a regression coefficient higher than 0.998, and quantification of the analyte was extrapolated from the curve.

Analyte recovery was estimated to be 89% for samples containing TCC at 50 μg/L, while was estimated to be 93% for samples containing TCC at 5 μg/L.

In our experiments, we were exploring 5–50 μg/L range of concentrations and in the standard curve, we tested a confidence interval ranging from 3 to 78 μg/L. In all these measures the quality was matching the limits for LOD (3 times sample signal over baseline sample) and LOQ (10 times sample signal over baseline sample). Consequently, the analytical method is satisfactory for the determination of TCC in this work.

2.4. Histology of the eye

2.4.1. 4-dpf larvae

Ten zebrafish larvae for each condition were fixed overnight in 4% formalin in PBS. Then they were gradually dehydrated in ascending concentrations of ethanol, following the methods reported by Sullivan-Brown et al. (2011) (Sullivan-Brown et al., 2011), and then placed in Bio Clear and embedded in paraffin for 4 μm thick sections (for details see Table S1). The retinal layers investigated were: retinal pigment epithelium (RPE), outer nuclear layer (ONL), outer plexiform layer (OPL), inner nuclear layer (INL), inner plexiform layer (IPL), retinal ganglion cell layer (RGL). Moreover, attention was focused on the morphology of ciliary marginal zone (CMZ).

2.4.2. 20-dpf larvae

Ten zebrafish larvae for each condition were placed for 24 h at 4 °C in Davidson's solution, whose formulation was reported in Fournie et al. (2000) (Fournie et al., 2000). To maximize the quality of sections, after fixation, fish were rinsed in 1X PBS and placed in 0.35 EDTA pH 7.8 for three days for decalcification. Then, they were rinsed once in 1X PBS, and gradually dehydrated in ascending concentrations of ethanol, and placed in Bio Clear, before being embedded in paraffin for 6 μm thick sections (for details see Table S1). The retinal layers investigated were: RPE, photoreceptor layer (PRL), ONL, OPL, INL, IPL, and RGL.

The protocol for haematoxylin and eosin staining for the larvae at 4- and 20-dpf is reported in Table S2. Images were captured with a Zeiss Axio Imager A2 microscope with Axiocam color 305 camera (Carl Zeiss Microscopy, Thornwood, NY) run by the Zen Blue software (Carl Zeiss Microscopy, Thornwood, NY). The evaluation of retinal layer thickness and the density of cells in larval ganglion cell layer (larvae at 4 dpf) were performed by means of Image J software (Rasband, W·S., ImageJ, U. S. National Institutes of Health, Bethesda, Maryland, USA).

2.5. Real-Time PCR

2.5.1. 4-dpf larvae

Three biological replicates were collected. The head was detached from the trunk cutting just anterior to the pectoral fin. In each replicate, fifty zebrafish heads for each condition were homogenized with 200 μL of Trizol™ Reagent (Invitrogen, CA, USA). Nucleic acid purity and RNA concentration were determined by NanoDrop™ 2000 Spectrophotometer (Thermo Fisher Scientific, DE, USA) and Qubit 2.0 fluorometer (Invitrogen, CA, USA), respectively. Concentrations of RNA samples and $A_{260/280}$ were reported in Table S3 cDNA was synthesized using SuperScript™ IV VILO™ ezDNase™ Enzyme (Invitrogen, Life Technologies Corporation, CA, USA) according to the manufacturer's instructions. Real-Time PCRs were performed with CFX Opus 96 Real-Time PCR system (Bio-rad, CA, USA) using Sso Advanced™ Universal Probes Supermix (Bio-rad, CA, USA) and gene-specific probes (Bio-rad, CA, USA) for microphthalmia-associated transcription factor (*mitfb*) (ID: qDreCIP0031120) and paired box gene 6a (*pax6a*) (ID: qDreCEP0046155). Mitfb is a key intrinsic mediator of RPE specification and plays a significant role in retina development (Ma et al., 2019). Pax6a is essential for the proper development of the optic vesicle and is required to maintain retinal progenitors in a proliferative state as well as to regulate the timing of cellular differentiation (Grindley et al., 1995; Lakowski et al., 2007).

The amplification procedure was the following: 95 °C × 3 min, then 40 cycles of 15 s denaturation at 95 °C and 1 min annealing/extension at 60 °C. The results were normalized using *β-actin* (qDreCEP0045468) as the reference gene. We used the $2^{-\Delta\Delta Ct}$ method to calculate the expression levels (Livak and Schmittgen, 2001).

2.5.2. 20-dpf larvae

Three biological replicates were used. The head was detached from the trunk cutting just anterior to the pectoral fin. In each replicate, six zebrafish heads for each condition were pooled to perform RNA extraction with Trizol™ Reagent. Determination of RNA concentration and purity (Table 4), cDNA synthesis and Real-Time PCR were performed as reported above for larvae at 4 dpf. The gene specific probes used were reported above.

2.6. Behavioral test on visual discrimination abilities

We measured subjects' visual discrimination ability by observing their spontaneous preference in a dichotomous choice between two visual stimuli (Gatto et al., 2021). This test required the larvae with an extended behavioral repertoire and was therefore conducted at the age of 20 dpf. Based on effect sized of a prior study (Merola et al., 2020b), we attempted to observe approximately 20 subjects per treatment. Due to subjects' availability, the sample size of this experiment was as follow: TCC 5 μg/L = 22; TCC 50 μg/L = 17; solvent control = 25. To conduct the test, each subject was moved into a 15 × 5 × 5 cm white plastic apparatus (Lucon-Xiccato et al., 2020), filled with 3 cm of dilution

water. A LED strip provided uniform illumination from above. In the two short walls of the apparatus, two visual stimuli were provided: a black triangle (side 0.86 cm, height 0.72 cm) and a black circle (Ø 0.62 cm). The surface area of the stimuli was the same. The position of the stimuli was randomly switched between the short walls of the apparatus across subjects.

The subjects could freely explore the stimuli for 10 min period, during which we recorded their behavior from above. The behavior was then analyzed from the recordings played back on a computer by an experimenter blind of the treatment of each subject. The behavioral analysis was conducted with the custom software 'Ciclic timer', which permitted us to associate each area of the apparatus to a separate, digital stopwatch. The experimenter calculated the time spent by each subject close to each stimulus, considering a choice area within 2.5 cm from the wall of the apparatus with the stimulus. The time spent close to the two stimuli was used to calculate an index of preference that allowed us to study visual discrimination (see Statistical analysis). The experimenter also recorded the time spent in the center of the apparatus, outside the choice areas of the two stimuli. This variable was used as control to ensure that the subjects did not spend the entire testing time far from both stimuli, which would prevent us to reliably calculate an index of preference. Based on the early studies (Gatto et al., 2021), we predicted to observe subjects from the TCC treatments to fail to discriminate between the visual stimuli presented and therefore, to express no behavioral preference in the test.

2.7. Statistical analysis

For the determination of TCC concentration, results were expressed as means ± SD. Statistical analyses were performed using the GraphPad Prism 7 software (GraphPad software). *t*-test was used to determine the statistical difference between TCC exposure solution without and with embryos. For the determination of retina layer thickness, cell density in retinal ganglion layer, and Real-Time PCR, results were expressed as the mean ± SEM. The assessment of normality was conducted using Shapiro-Wilk test. Real time data were analyzed by Kruskal-Wallis's test followed by Dunn's post-hoc comparisons. Differences were considered statistically significant if p values were * $p < 0.05$; ** $p < 0.005$; *** $p < 0.0005$.

Analysis of behavioral data was performed in R version 3.2.2 (The R Foundation for Statistical Computing, Vienna, Austria, http://www.r-project.org). We focused on two dependent variables. We initially compared the time spent by subjects from the different treatment in the central, no-choice area of the apparatus with ANOVA. This was a control variable that described whether the fish noticed and approached the two stimuli. It was not expected to vary between experimental treatments otherwise it would make it difficult to interpret the following variable. We then analyzed the main depended variable, an index of preference for one of the two stimuli. We calculated this index in favor of the circle as: time spent in the choice area of circle/(time spent in the choice area of circle + time spent in the choice area of triangle). The index ranged from 0 to 1, with increasing values indicating greater preference for the circle stimulus. The index was analyzed with one-sample t-tests against the index value indicating a random choice between the stimuli (0.5). A significant outcome would indicate that a group of subjects displayed a significant preference for one of the stimuli, and therefore were able to discriminate them. Five outliers from the TCC 5 μg/L treatment and 1 outlier from the TCC 50 μg/L treatment were removed to meet test's assumptions. Outliers were identified by calculating the threshold value corresponding to 1.5 times the interquartile range below and above of the 25th and the 75th percentile of the data distribution, respectively (Walfish, 2006).

3. Results

3.1. 4-dpf larvae

3.1.1. Chemical analyses

The amount of TCC in the solutions with and without embryos is shown in Table 2.

At the lower tested concentration data reported in Table 2 showed a not significant difference between samples with or without embryos (4 dpf), while at the higher concentration a significant difference of 15% between the presence or the absence of embryos was observed. These data are similar to those obtained by Chen et al. (2021) in terms of recovery of TCC from water in the presence of embryos at low (5 μg/L) and high (50 μg/L) being respectively more than 100% (with respect to the nominal concentration) and 85% at 96 h. The TCC concentration in the solutions with the embryos were lower than the corresponding nominal concentrations suggesting an uptake by the larvae or a possible degradation of TCC.

3.1.2. Histology of the eye

Larvae exposed to both concentrations of TCC showed differences in retinal morphology compared to solvent control (Fig. 1). First, INL and IPL were significantly decreased at both concentrations of TCC ($p < 0.0005$) compared to solvent control (Fig. 1 a, c). RGL showed a significant increase in thickness ($p < 0.005$ for TCC 5 and $p < 0.0005$ for TCC 50) (Fig. 1 a,d), which corresponds to a significant decrease in RGL density ($p < 0.0005$ at both concentrations) (Fig. 1 a, e-f). In fact, the ganglion cell count demonstrated a significantly decrease of cell density in treated embryos (Fig. 1 f). In addition to the evident microphthalmia, the CMZ appeared less organized in treated larvae (framed in red, Fig. 1 a-b).

3.1.3. Real-Time PCR

The analysis revealed a significant decrease ($p < 0.05$) in *mitfb* and *pax6a* gene expression levels at the lower concentration, while at higher concentration we observed only a slight negative trend in expression level (Fig. 2).

3.2. 20 dpf larvae

3.2.1. Histology of the eye

At 20 dpf, zebrafish larvae exposed to the three treatments in their early life showed no changes in the eyes (Fig. 2a). The morphology of retinal layers appeared normal (Fig. 3b). However, following exposure to either concentration of TCC, increased the thickness of the IPL (*$p < 0.05$), while only lower concentration altered PRL thickness (*$p < 0.05$) (Fig. 2d).

3.2.2. Real-Time PCR

The gene expression analysis showed a significant increase of *mitfb* levels at lower concentration (*$p < 0.05$) compared to solvent control. *Pax6a* did not undergo any changes (Fig. 4 a).

Table 2
TCC concentrations found in the zebrafish test solutions.

TCC nominal concentration (μg/L)	TCC concentration without embryos (μg/L)		TCC concentration with embryos (μg/L)		Significance
	Mean	SD	Mean	SD	
5	4.03	0.33	3.62	0.38	P = 0.2016
50	48.92	0.83	33.09	3.5	P = 0.0016

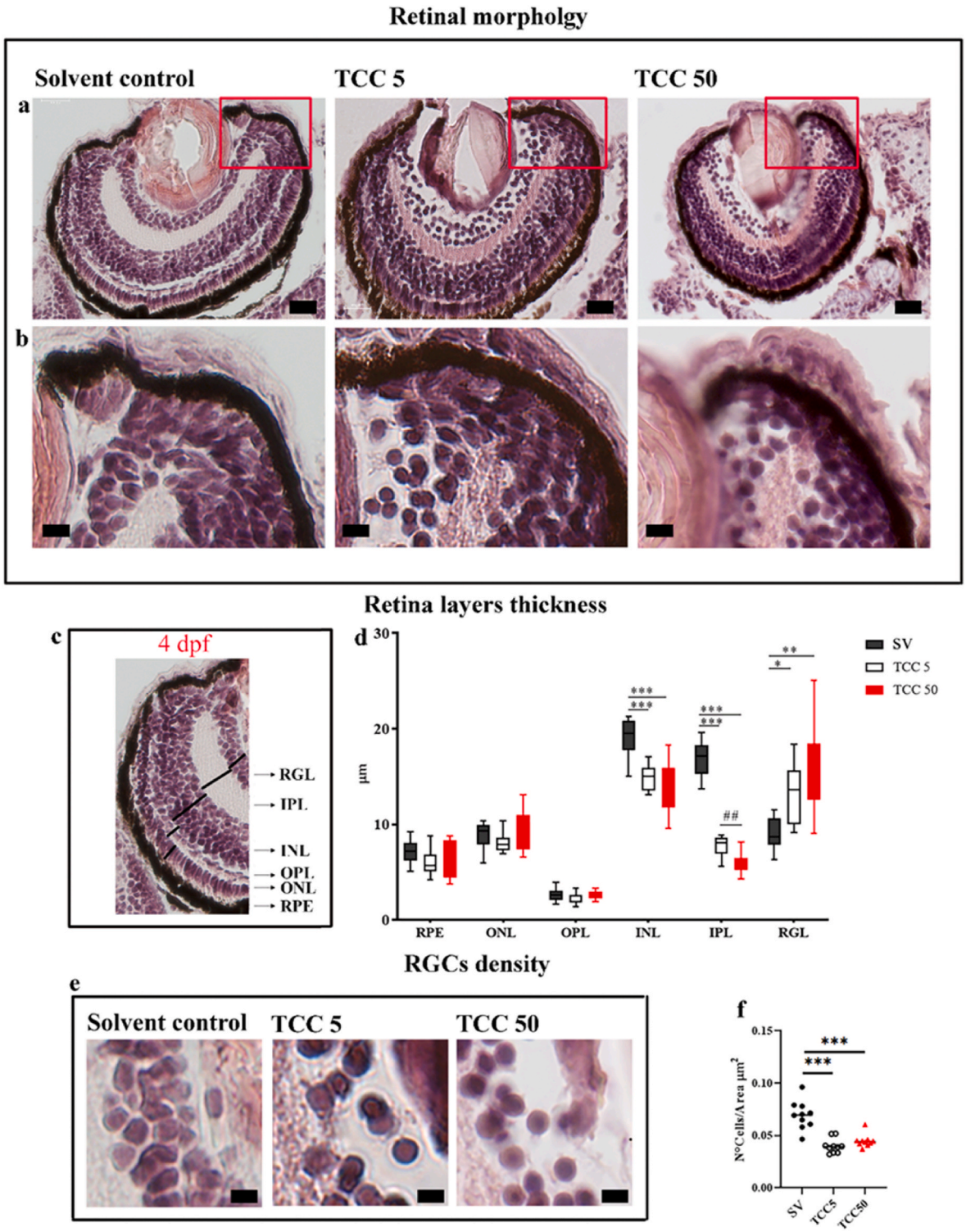

Fig. 1. Results of the analysis performed on 4-dpf larvae. a) Representative images of zebrafish eyes with haematoxylin and eosin staining. Framed in red CMZ. 0,01% DMSO is the Solvent control. Scale bar 20 µm. b) Magnification of CMZ to appreciate the morphological changes. Scale bar 7 µm. c) Retinal organization in 4-dpf larvae. d) Measure of retina layers thickness. Statistical differences are indicated as * $p < 0.05$, ** $p < 0.005$ and *** $p < 0.0005$ vs. DMSO, or as $^{\#\#}p < 0.005$ vs. TCC 5. e) Magnification of RGL to appreciate the cell organization. Scale bar 7 µm. f) Cell density in RGL, measured as number of cells/area (µm^2). Statistical differences are indicated as *** $p < 0.0005$ vs. solvent control. (The results are expressed as mean ± SEM). Abbreviations: SV, solvent control; CMZ, ciliary marginal zone; RPE, retinal pigment epithelium; ONL, outer nuclear layer; OPL outer plexiform layer; INL, inner nuclear layer; IPL, inner plexiform layer; RGL, retinal ganglion cell layer.

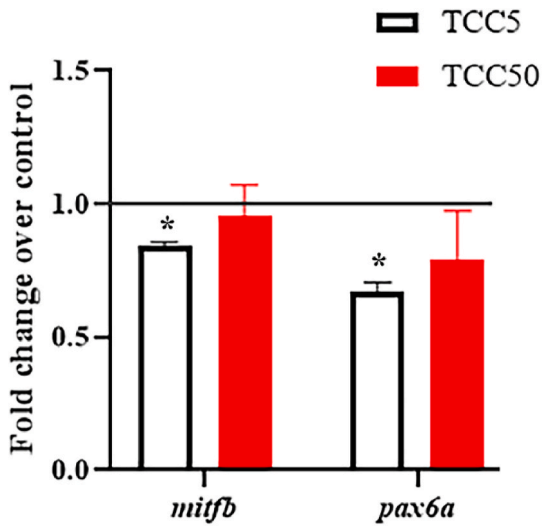

Fig. 2. Gene expression analysis of *mitfb* and *pax6a*. Statistical differences are indicated as * $p < 0.05$ vs. solvent control. (The results are expressed as mean ± SEM).

3.2.3. *Visual discrimination abilities*

In the visual discrimination test, subjects from the different treatments did not differ in engaging the stimuli, spending a similar amount of time in the center of the apparatus (ANOVA: $F_{2,55} = 1.218$, $p = 0.304$). This indicated that the treatment did not determine major changes in swimming patterns of the subjects and their general response towards the stimuli. However, subjects of the different treatment showed different discrimination performance as indicated by the analysis of the preference index (Fig. 4 b): control larvae exposed to the solvent spent significantly more time close to the triangle stimulus (one-sample *t*-test: $t_{24} = 2.165$, $p = 0.041$), indicating the ability to perform the discrimination between the two stimuli presented. Conversely, discrimination between the two stimuli was not significant in larvae exposed to TCC 5 μg/L ($t_{20} = 1.265$, $p = 0.220$) and TCC 50 μg/L ($t_{11} = 1.266$, $p = 0.232$).

4. Discussion

Retinogenesis is highly conserved among vertebrates so that even in divergent phyla, such as teleosts and mammals, it is governed by a similar interplay between extrinsic and intrinsic influences and additionally, the retinae show a similar structure (Kitambi et al., 2011). These similarities make zebrafish a suitable model for studying the eye formation changes induced by external factors in vertebrates. It is worth noting that the eye represents an highly sensitive target to chemical

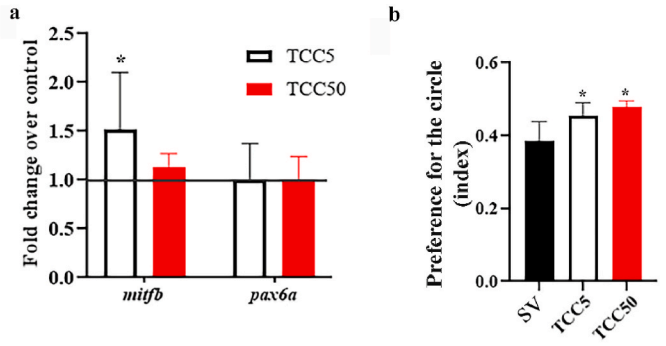

Fig. 4. a) Gene expression analysis of mitfb and pax6a. Statistical differences are indicated as * $p < 0.05$ vs. solvent control. (The results are expressed as mean ± SEM). b) Visual discrimination performance of the subjects measured as preference for the circle stimulus versus the triangle stimulus (mean ± standard error) in the behavioral test. Asterisks indicate significant deviance from random choice (0.5 preference for the circle). *$p < 0.05$.

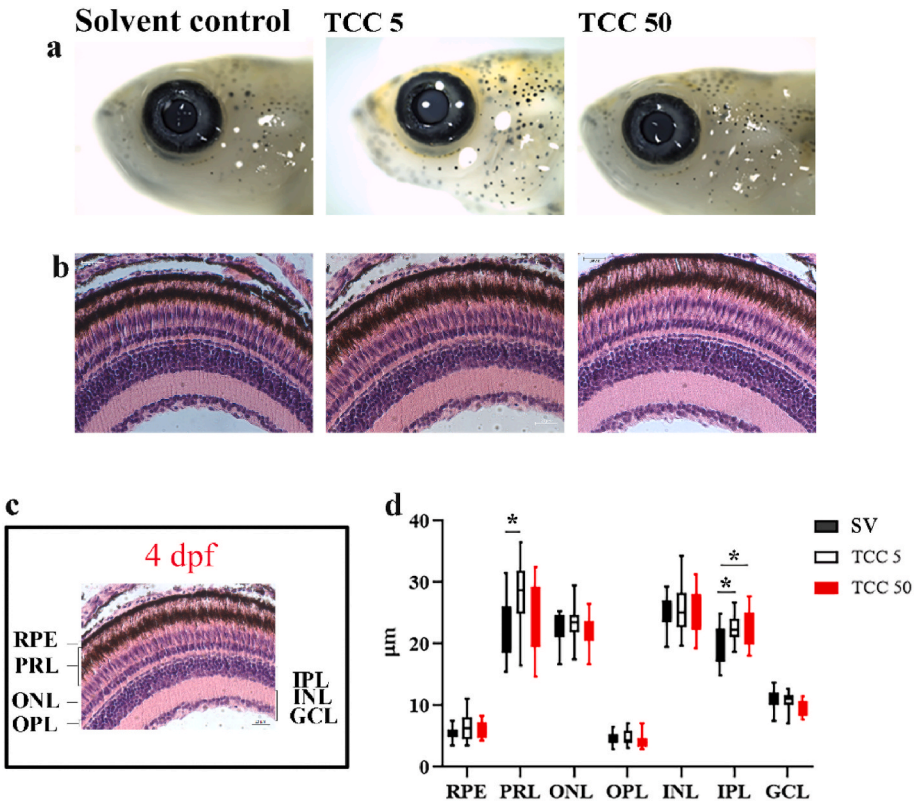

Fig. 3. a) Results of the analysis performed on 20-dpf larvae. a) Representative images of zebrafish eyes. b) Representative images of zebrafish eyes with haematoxylin and eosin staining. Scale bar 20 μm. RPE, retinal pigment epithelium; PRL, photoreceptor layer; ONL, outer nuclear layer; OPL outer plexiform layer; INL, inner nuclear layer; IPL, inner plexiform layer; RGL, retinal ganglion cell layer. c) Retinal organization in 20-dpf larvae. d) Measure of retina layers thickness. Statistical differences are indicated as * $p < 0.05$ vs. solvent control (SV). The results are expressed as mean ± SEM.

exposure. For example, a range of xenobiotics, such as the thyroid hormone disruptors (TD) propylthiouracil and tetrabromobisphenol A, could lead to morphological and physiological changes of eyes in zebrafish larvae (Baumann et al., 2016). TCC is a TD and we observed that it induces impaired eye development and visual functions; as well as other well-known thyroid axis disruptors. The starting point of this study is represented by the evaluation of retinal morphology in solvent controls and specimens exposed to TCC (Fig. 1 a-b). Observing sections from treated larvae at 4-dpf, the loss of a clear division between the retina layers can be noticed. In particular, the INL and IPL have a lower thickness in exposed larvae, and their size correlates with the concentrations used (Fig. 1d). The INL contains the nuclear bodies of bipolar, horizontal, amacrine cells and Müller glial cells (Gollisch and Meister, 2010). The main function of INL is to transmit the information from photoreceptors to ganglion cells, while Müller glial cells have a role in maintaining retinal homeostasis. The IPL includes the synaptic connections between the axons of bipolar and amacrine interneurons and the dendrites of ganglion cells (Angueyra and Kindt, 2018). The retinal patterning alterations observed might be explained by defects in retinal cell development that influence cell proliferation and migration. In light of the above, we hypothesize that TCC could influence retinogenesis acting on the CMZ. In fact, the CMZ morphology of 4-dpf treated larvae appeared abnormal in comparison with control specimens (Fig. 1b). This region is responsible for retinal neurogenesis, and contributes to maintaining the tissue architecture. One of the first studies conducted by Wetts et al. (1989) on frogs showed that this region contained retinal stem cells and retinal progenitor cells (Wetts et al., 1989). More recent extensive works gave information about the role of CMZ in zebrafish, which collaterally develops during the early phase of the rapid proliferation of cells (Angileri and Gross, 2020). Thus, by 3 dpf at the retina's periphery, there are undifferentiated and diving cells opposing the other cells that exited the cell cycle to differentiate (Wan et al., 2016). The retinal stem cells in the CMZ represent the stem niche, contributing to retinal progenitors' generation (Todd et al., 2016). Pax6 is required for the retina's normal development, to maintain progenitors' proliferation. In particular, the *pax6a* isoform is expressed in the lens and in retinal stem cells and progenitors, while the isoform *pax6b* is prevalent in the developing pancreas (Thisse and Thisse, 2004). The *pax6a* levels decrease at the end of exposure in the 4-dpf larvae exposed at lower concentration (Fig. 1g), although it did not change for higher concentration. The decrease in RGL's density is observed at both concentrations in the larvae at 4 dpf (Fig. 1 e, f). The ganglion cells represent the final output since their axons converge in the optic nerve formation. Among the first events of retinogenesis, there is the generation of retinal ganglion cells, which firstly become post-mitotic cells, with the final divisions between 1 and 1.5 dpf (Gollisch and Meister, 2010). The damage in this layer corroborated the hypothesis that the injury may influence the CMZ, altering all the subsequent steps. However, it must be emphasized that the differentiation of retinal ganglion cells also depends on the presence of extrinsic factors, which control the fate of these cells (Nguyen-Ba-Charvet and Rebsam, 2020).

Regarding intrinsic factors, *mitfb* is a key mediator of RPE specification and retina development. Ma et al. (2019) showed in their study on *mitfb* mutant mice that RPE appeared as a pseudostratified epithelium with altered pigmentation and retinal degeneration (Ma et al., 2019). In our research, *mitfb* levels decreased with significance at lower concentration (Fig. 2) in 4-dpf larvae, and the RPE layer, particularly in TCC 5 μg/L, appeared less pigmented and with altered morphology, suggesting an impairment also in this layer that plays a critical role for retina physiology.

Overall, these first collected data highlight that environmentally relevant concentrations of TCC produced phenotypic defects of the retina, in agreement with Chen et al. (2021) (Chen et al., 2021). Moreover, these data showed that TCC modulated the expression levels of key genes implicated in retina development. Surprisingly, *mitfb* and *pax6a* gene expression was significantly modulated only by the lowest concentration highlighting concentration effects on retinal cells' response.

Although the highest concentration induced more marked defects in retina morphology and eyes size (eye length and wide), the expression of the two master's gene of retina development did not change significantly, we hypothesize that the greater damage produces a major retinal regenerative response as proposed also by Raymond et al. (1988) (Raymond et al., 1988). The findings of our study could be explained by a favorable response resulting from the acute toxicity which occurred in the initial stages of development (Wang et al., 2022). It is only a hypothesis, for which further investigations are needed.

To assess the eventual recovery from the injury or long-term effects, we performed investigations at 20 dpf. In contrast to mammals, zebrafish can regenerate all retinal cell types using the source of stem cells maintained in the CMZ (see above) (Wan and Goldman, 2016). Several regeneration pathways have been clarified, and much attention was given to the role of Müller glia cells (Wan and Goldman, 2016). These are so responsive in case of damage that allow for reestablishing retinal homeostasis and *pax6*-related pathways seem to be involved (Thummel et al., 2008, 2010). The eyes size and histological sections of 20-dpf larvae (Fig. 3 a,b) suggest an improvement compared to the early larval damage observed. For example, in our study, a reduction in the thickness of retinal layers cannot be observed (Fig. 2d). In fact, as a response to the alterations induced by TCC, PRL, and IPL appeared to increase at one or both concentrations (Fig. 3 c,d). The increase of retinal layers may be explained by a compensative mechanism that tries to restore a physiological condition. For example, RPE is a single layer of cells that separates the retina from the choroid. It consists of pigment-containing cells and supports the visual function, interacting with the outer segment of photoreceptors by means of long apical microvilli (Strauss, 2005). RPE sustains the process of retinogenesis, producing some critical factors which stimulate cell proliferation and the reestablishment of retinal architecture (Steele et al., 1993; Tanihara et al., 1997). In our study, larvae that were exposed at early stages to TCC 5 μg/L present the increment of *mitfb* gene expression levels, suggesting a chemical-induced stimulation to recovery. PRL contains the outer segment of photoreceptors, and we observed its increased thickness at lower concentration. Further investigations should be performed to assess whether the increase in thickness is related to changes in outer segment length, since the literature offers examples of correlations between these kinds of modifications and visual acuity (Forooghian et al., 2010; Maden et al., 2017) or defects in RPE-mediated phagocytosis (Mukherjee et al., 2007; Mazzoni et al., 2014).

The larvae at 20 dpf also showed an increment in IPL. IPL is composed of a dense reticulum of cells in a multilayers structure. This stratification is present both in the larval stages and the adults (Nevin et al., 2008). The IPL of the vertebrate retina is the best example of a multilayered synaptic neuropil region. In this layer, the dendrites of RGC stratify and form contact with axons of bipolar cells that deliver information from the photoreceptors. Moreover, RGC dendrites do synapsis with inhibitory interneurons and amacrine cells (Gollisch and Meister, 2010). The heterogeneity and complexity of IPL make it challenging to formulate a hypothesis. However, the increased size of IPL suggests possible defects in visual information transmission.

To confirm the long-term effects of exposure to TCC, we looked directly at the behavioral output related to the visual system, investigating the ability to perform visual discriminations in zebrafish larvae. In our test, we exploited the spontaneous preference of larvae for specific visual stimuli, which can be investigated in a controlled setting in the laboratory (Gatto et al., 2021). When presented with the choice between a triangle stimulus and a circle, larvae usually approach the former and avoid the second shape, which might be perceived as the eye of a larger and potentially, a predator fish. In the present study, we found that TCC impaired this shape discrimination ability: while control larvae expressed the expected preference for the triangle shape, specimens early exposed to TCC did not. This effect was not explained by

differences in engaging the stimuli, which was similar across the experimental groups. Indeed, we found no significant effect of treatment in time spent in the center of the apparatus (i.e., far from both stimuli). Thus, the subjects noticed and showed a similar general attraction towards the visual stimuli. We conclude that TCC caused an anomalous behavior due to an alteration in visual functions that prevented fine recognition of subtle differences between stimuli. It is worth noting that the preference for the triangle, and therefore the discrimination capacity, was absent on subjects exposed to both TCC concentrations. It appears that the effect of TCC on visual capacities was present even at low, environmentally relevant concentrations. For many species, visual discrimination ability is a fundamental requirement in nature, allowing the recognition of the main biological stimuli. Research has shown that in nature, zebrafish probably use vision to recognize social companions (Spence and Smith, 2007), reproductive partners (Turnell et al., 2003), predators (Barcellos et al., 2007), and prey (Howe et al., 2018). Our visual discrimination test has not been directly related to such activities. However, it is plausible that the visual impairment due to TCC could have some consequences when fish perform such activities in their natural environment.

This study is a preliminary approach to evaluating the effects of early exposure to TCC on zebrafish larval retina morphology. We tried to distinguish between the alterations at the end of exposure (performing the analysis at 4 dpf) and the delayed effects, testing the larvae at 20 dpf. A more comprehensive explanation will need the study of particular mechanisms or pathways, starting from the data obtained. Except for the immunological role of TCC (Wei et al., 2018) and some information concerning the thyroid hormone disrupting activity (Hinther et al., 2011; Wu et al., 2016b), there is a lack of knowledge about the effects of TCC on zebrafish larvae and humans. Particularly for human health, the research of these topics is crucial. For instance, the discovery of TCC in maternal urine and cord blood raised serious concerns about its potential impact on human development. Using an environmentally relevant concentration (5 μg/L) allowed us to understand the risks associated with the exposure, although there is still much to investigate. The data found in this study showed that early exposure to TCC negatively influences eyes' development and consequently zebrafish visually-driven behavior.

5. Conclusions

This study provided preliminary results of the effects deriving from the exposure to environmentally relevant concentrations of TCC on fish ocular development. In particular, the results allowed only an exploratory description of the events, while an analysis of molecular mechanisms and underlined pathways represent the following step for a better comprehension of the toxicological effects. However, these considerations may contribute to the risk assessment of TCC, resulting in an increased awareness of the impact of personal care products (and their particular ingredients or additives) on human health.

Credit author statement

Elisabetta Benedetti and Monia Perugini: Conceptualization, Writing – original draft, Funding acquisition. Giulia Caioni and Carmine Merola contributed equally to this work: Investigation, Formal analysis. Cristiano Bertolucci, Tyrone Lucon-Xiccato and Beste Başak Savaşçı; : Writing – review & editing. Michele d'Angelo and Nunzio Antonio Cacciola: Formal analysis. Mara Massimi, Martina Colasante and Rodolfo Ippoliti: Data curation. Giulia Fioravanti: Investigation, Formal analysis.

Declaration of competing interest

The authors declare that they have no known competing financial interests or personal relationships that could have appeared to influence the work reported in this paper.

Data availability

Data will be made available on request.

Acknowledgements

We have no competing interests. We are thankful to Andrea Margutti for building the apparatuses of the behavioral tests. Fundings were provided by FFO BenedettiUnivaq, and FAR UniFE.

Appendix A. Supplementary data

Supplementary data to this article can be found online at https://doi.org/10.1016/j.chemosphere.2023.138348.

References

Ahn, K.C., Zhao, B., Chen, J., Cherednichenko, G., Sanmarti, E., Denison, M.S., Lasley, B., Pessah, I.N., Kültz, D., Chang, D.P.Y., Gee, S.J., Hammock, B.D., 2008. In vitro biologic activities of the antimicrobials triclocarban, its analogs, and triclosan in bioassay screens: receptor-based bioassay screens. Environ. Health Perspect. 116, 1203–1210. https://doi.org/10.1289/ehp.11200.

Angileri, K.M., Gross, J.M., 2020. dnmt1 function is required to maintain retinal stem cells within the ciliary marginal zone of the zebrafish eye. Sci. Rep. 10, 11293 https://doi.org/10.1038/s41598-020-68016-z.

Angueyra, J.M., Kindt, K.S., 2018. Leveraging zebrafish to study retinal degenerations. Front. Cell Dev. Biol. 6, 110. https://doi.org/10.3389/fcell.2018.00110.

Azzouz, A., Rascón, A.J., Ballesteros, E., 2016. Simultaneous determination of parabens, alkylphenols, phenylphenols, bisphenol A and triclosan in human urine, blood and breast milk by continuous solid-phase extraction and gas chromatography-mass spectrometry. J. Pharm. Biomed. Anal. 119, 16–26. https://doi.org/10.1016/j.jpba.2015.11.024.

Barcellos, L.J.G., Ritter, F., Kreutz, L.C., Quevedo, R.M., da Silva, L.B., Bedin, A.C., Finco, J., Cericato, L., 2007. Whole-body cortisol increases after direct and visual contact with a predator in zebrafish, *Danio rerio*. Aquaculture 272, 774–778.

Baumann, L., Ros, A., Rehberger, K., Neuhauss, S.C.F., Segner, H., 2016. Thyroid disruption in zebrafish (Danio rerio) larvae: different molecular response patterns lead to impaired eye development and visual functions. Aquat. Toxicol. 172, 44–55. https://doi.org/10.1016/j.aquatox.2015.12.015.

Caioni, G., d'Angelo, M., Panella, G., Merola, C., Cimini, A., Amorena, M., Benedetti, E., Perugini, M., 2021. Environmentally relevant concentrations of triclocarban affect morphological traits and melanogenesis in zebrafish larvae. Aquat. Toxicol. 236, 105842 https://doi.org/10.1016/j.aquatox.2021.105842.

Cao, L.-Y., Xu, Y.-H., He, S., Ren, X.-M., Yang, Y., Luo, S., Xie, X.-D., Luo, L., 2020. Antimicrobial triclocarban exhibits higher agonistic activity on estrogen-related receptor γ than triclosan at human exposure levels: a novel estrogenic disruption mechanism. Environ. Sci. Technol. Lett. 7, 434–439. https://doi.org/10.1021/acs.estlett.0c00338.

Chalew, T.E., Halden, R.U., 2009. Environmental exposure of aquatic and terrestrial biota to triclosan and triclocarban. J. Am. Water Works Assoc. 45, 4–13. https://doi.org/10.1111/j.1752-1688.2008.00284.x.

Chen, X.-F., Chen, Z.-F., Lin, Z.-C., Liao, X.-L., Zou, T., Qi, Z., Cai, Z., 2021. Toxic effects of triclocarban on larval zebrafish: a focus on visual dysfunction. Aquat. Toxicol. 241, 106013 https://doi.org/10.1016/j.aquatox.2021.106013.

Coogan, M.A., Edziyie, R.E., La Point, T.W., Venables, B.J., 2007. Algal bioaccumulation of triclocarban, triclosan, and methyl-triclosan in a North Texas wastewater treatment plant receiving stream. Chemosphere 67, 1911–1918. https://doi.org/10.1016/j.chemosphere.2006.12.027.

Das Sarkar, S., Nag, S.K., Kumari, K., Saha, K., Bandyopadhyay, S., Aftabuddin, M., Das, B.K., 2020. Occurrence and safety evaluation of antimicrobial compounds triclosan and triclocarban in water and fishes of the multitrophic niche of river torsa, India. Arch. Environ. Contam. Toxicol. 79, 488–499. https://doi.org/10.1007/s00244-020-00785-0.

Forooghian, F., Stetson, P.F., Meyer, S.A., Chew, E.Y., Wong, W.T., Cukras, C., Meyerle, C.B., Ferris, F.L., 2010. Relationship between photoreceptor outer segment length and visual acuity in diabetic macular edema. Retina 30, 63–70. https://doi.org/10.1097/IAE.0b013e3181bd2c5a.

Fournie, J., Krol, R., Hawkins, W., 2000. Fixation of fish tissues. In: The Laboratory Fish, pp. 569–578. https://doi.org/10.1016/B978-012529650-2/50043-3.

Gatto, E., Bruzzone, M., Lucon-Xiccato, T., 2021. Innate visual discrimination abilities of zebrafish larvae. Behav. Process. 193, 104534 https://doi.org/10.1016/j.beproc.2021.104534.

Gollisch, T., Meister, M., 2010. Eye smarter than scientists believed: neural computations in circuits of the retina. Neuron 65, 150–164. https://doi.org/10.1016/j.neuron.2009.12.009.

Gomes, M.F., de Carvalho Soares de Paula, V., Rocha Martins, L.R., Esquivel Garcia, J.R., Yamamoto, F.Y., Martins de Freitas, A., 2021. Sublethal effects of triclosan and triclocarban at environmental concentrations in silver catfish (Rhamdia quelen)

embryos. Chemosphere 263, 127985. https://doi.org/10.1016/j.chemosphere.2020.127985.
Grindley, J.C., Davidson, D.R., Hill, R.E., 1995. The role of Pax-6 in eye and nasal development. Development 121, 1433–1442. https://doi.org/10.1242/dev.121.5.1433.
Halden, R.U., Paull, D.H., 2005. Co-occurrence of triclocarban and triclosan in U.S. Water resources. Environ. Sci. Technol. 39, 1420–1426. https://doi.org/10.1021/es049071e.
Halla, N., Fernandes, I.P., Heleno, S.A., Costa, P., Boucherit-Otmani, Z., Boucherit, K., Rodrigues, A.E., Ferreira, I.C.F.R., Barreiro, M.F., 2018. Cosmetics preservation: a review on present strategies. Molecules 23, E1571. https://doi.org/10.3390/molecules23071571.
Hinther, A., Bromba, C.M., Wulff, J.E., Helbing, C.C., 2011. Effects of triclocarban, triclosan, and methyl triclosan on thyroid hormone action and stress in frog and mammalian culture systems. Environ. Sci. Technol. 45, 5395–5402. https://doi.org/10.1021/es1041942.
Howe, H.B., McIntyre, P.B., Wolman, M.A., 2018. Adult Zebrafish primarily use vision to guide Piscivorous foraging behavior. Behav. Process. 157, 230–237.
Huang, H., Du, G., Zhang, W., Hu, J., Wu, D., Song, L., Xia, Y., Wang, X., 2014. The in vitro estrogenic activities of triclosan and triclocarban. J. Appl. Toxicol. 34, 1060–1067. https://doi.org/10.1002/jat.3012.
Iacopetta, D., Catalano, A., Ceramella, J., Saturnino, C., Salvagno, L., Ielo, I., Drommi, D., Scali, E., Plutino, M.R., Rosace, G., Sinicropi, M.S., 2021. The different facets of triclocarban: a review. Molecules 26, 2811. https://doi.org/10.3390/molecules26092811.
Kitambi, S.S., Chandrasekar, G., Addanki, V.K., 2011. Teleost fish – powerful models for studying development, function and diseases of the human eye. Curr. Sci. 100, 1815–1823.
Lakowski, J., Majumder, A., Lauderdale, J.D., 2007. Mechanisms controlling Pax6 isoform expression in the retina have been conserved between teleosts and mammals. Dev. Biol. 307, 498–520. https://doi.org/10.1016/j.ydbio.2007.04.015.
Livak, K.J., Schmittgen, T.D., 2001. Analysis of relative gene expression data using real-time quantitative PCR and the 2(-Delta Delta C(T)) Method. Methods 25, 402–408. https://doi.org/10.1006/meth.2001.1262.
Lucon-Xiccato, T., De Russi, G., Bertolucci, C., 2020. A novel-odour exploration test for measuring anxiety in adult and larval zebrafish. J. Neurosci. Methods 335, 108619. https://doi.org/10.1016/j.jneumeth.2020.108619.
Ma, X., Li, H., Chen, Y., Yang, J., Chen, H., Arnheiter, H., Hou, L., 2019. The transcription factor MITF in RPE function and dysfunction. Prog. Retin. Eye Res. 73, 100766 https://doi.org/10.1016/j.preteyeres.2019.06.002.
Maden, G., Cakir, A., Icar, D., Erden, B., Bolukbasi, S., Elcioglu, M., 2017. The distribution of the photoreceptor outer segment length in a healthy population. Journal of Ophthalmology 2017, e4641902. https://doi.org/10.1155/2017/4641902.
Mazzoni, F., Safa, H., Finnemann, S.C., 2014. Understanding photoreceptor outer segment phagocytosis: use and utility of RPE cells in culture. Exp. Eye Res. 51–60. https://doi.org/10.1016/j.exer.2014.01.010.
Merola, C., Lai, O., Conte, A., Crescenzo, G., Torelli, T., Alloro, M., Perugini, M., 2020a. Toxicological assessment and developmental abnormalities induced by butylparaben and ethylparaben exposure in zebrafish early-life stages. Environ. Toxicol. Pharmacol. 80, 103504 https://doi.org/10.1016/j.etap.2020.103504.
Merola, C., Perugini, M., Conte, A., Angelozzi, G., Bozzelli, M., Amorena, M., 2020b. Embryotoxicity of methylparaben to zebrafish (*Danio rerio*) early-life stages. Comp. Biochem. Physiol. C Toxicol. Pharmacol. 236, 108792 https://doi.org/10.1016/j.cbpc.2020.108792.
Mukherjee, P.K., Marcheselli, V.L., de Rivero Vaccari, J.C., Gordon, W.C., Jackson, F.E., Bazan, N.G., 2007. Photoreceptor outer segment phagocytosis attenuates oxidative stress-induced apoptosis with concomitant neuroprotectin D1 synthesis. Proc. Natl. Acad. Sci. USA 104, 13158–13163. https://doi.org/10.1073/pnas.0705963104.
Nevin, L.M., Taylor, M.R., Baier, H., 2008. Hardwiring of fine synaptic layers in the zebrafish visual pathway. Neural Dev. 3, 36. https://doi.org/10.1186/1749-8104-3-36.
Nguyen-Ba-Charvet, K.T., Rebsam, A., 2020. Neurogenesis and specification of retinal ganglion cells. Int. J. Mol. Sci. 21, 451. https://doi.org/10.3390/ijms21020451.
Prosser, R.S., Lissemore, L., Topp, E., Sibley, P.K., 2014. Bioaccumulation of triclosan and triclocarban in plants grown in soils amended with municipal dewatered biosolids. Environ. Toxicol. Chem. 33, 975–984. https://doi.org/10.1002/etc.2505.
Pycke, B.F.G., Geer, L.A., Dalloul, M., Abulafia, O., Jenck, A.M., Halden, R.U., 2014. Human fetal exposure to triclosan and triclocarban in an urban population from brooklyn, New York. Environ. Sci. Technol. 48, 8831–8838. https://doi.org/10.1021/es501100w.
Raymond, P.A., Reifler, M.J., Rivlin, P.K., 1988. Regeneration of goldfish retina: rod precursors are a likely source of regenerated cells. J. Neurobiol. 19, 431–463. https://doi.org/10.1002/neu.480190504.
Schebb, N.H., Inceoglu, B., Ahn, K.C., Morisseau, C., Gee, S., Hammock, B.D., 2011. Investigation of human exposure to triclocarban after showering, and preliminary evaluation of its biological effects. Environ. Sci. Technol. 45, 3109–3115. https://doi.org/10.1021/es103650m.
Shi, Y., Liu, X., Zhang, J., Shao, B., 2013. Analysis of triclosan and triclocarban in human nails using isotopic dilution liquid chromatography-tandem mass spectrometry. J. Chromatogr., B: Anal. Technol. Biomed. Life Sci. 934, 97–101. https://doi.org/10.1016/j.jchromb.2013.07.003.
Spence, R., Smith, C., 2007. The role of early learning in determining shoaling preferences based on visual cues in the zebrafish, *Danio rerio*. Ethology 113, 62–67.
Steele, F.R., Chader, G.J., Johnson, L.V., Tombran-Tink, J., 1993. Pigment epithelium-derived factor: neurotrophic activity and identification as a member of the serine protease inhibitor gene family. Proc. Natl. Acad. Sci. U. S. A. 90, 1526–1530. https://doi.org/10.1073/pnas.90.4.1526.
Strauss, O., 2005. The retinal pigment epithelium in visual function. Physiol. Rev. 85, 845–881. https://doi.org/10.1152/physrev.00021.2004.
Sullivan-Brown, J., Bisher, M.E., Burdine, R.D., 2011. Embedding, serial sectioning and staining of zebrafish embryos using JB-4 resin. Nat. Protoc. 6, 46–55. https://doi.org/10.1038/nprot.2010.165.
Tanihara, H., Inatani, M., Honda, Y., 1997. Growth factors and their receptors in the retina and pigment epithelium. Prog. Retin. Eye Res. 16, 271–301. https://doi.org/10.1016/S1350-9462(96)00028-6.
Thisse, B., Thisse, C., 2004. Fast release clones: a high throughput expression analysis. ZFIN Direct Data Submission. http://zfin.org.
Thummel, R., Enright, J.M., Kassen, S.C., Montgomery, J.E., Bailey, T.J., Hyde, D.R., 2010. Pax6a and Pax6b are required at different points in neuronal progenitor cell proliferation during zebrafish photoreceptor regeneration. Exp. Eye Res. 90, 572–582. https://doi.org/10.1016/j.exer.2010.02.001.
Thummel, R., Kassen, S.C., Enright, J.M., Nelson, C.M., Montgomery, J.E., Hyde, D.R., 2008. Characterization of Müller glia and neuronal progenitors during adult zebrafish retinal regeneration. Exp. Eye Res. 87, 433–444. https://doi.org/10.1016/j.exer.2008.07.009.
Todd, L., Suarez, L., Squires, N., Zelinka, C.P., Gribbins, K., Fischer, A.J., 2016. Comparative analysis of glucagonergic cells, glia and the circumferential marginal zone in the reptilian retina. J. Comp. Neurol. 524, 74–89. https://doi.org/10.1002/cne.23823.
Turnell, E.R., Mann, K.D., Rosenthal, G.G., Gerlach, G., 2003. Mate choice in zebrafish (*Danio rerio*) analyzed with video-stimulus techniques. Biol. Bull. 205, 225–226.
Walfish, S., 2006. A review of statistical outlier methods. Pharmaceut. Technol. 30, 82.
Wan, J., Goldman, D., 2016. Retina regeneration in zebrafish. Curr. Opin. Genet. Dev. 40, 41–47. https://doi.org/10.1016/j.gde.2016.05.009.
Wan, Y., Almeida, A.D., Rulands, S., Chalour, N., Muresan, L., Wu, Y., Simons, B.D., He, J., Harris, W.A., 2016. The ciliary marginal zone of the zebrafish retina: clonal and time-lapse analysis of a continuously growing tissue. Development 143, 1099–1107. https://doi.org/10.1242/dev.133314.
Wang, Y., Li, W., Zhang, C., Peng, W., Xu, Z., 2022. RBM24 is localized to stress granules in cells under various stress conditions. Biochem. Biophys. Res. Commun. 608, 96–101. https://doi.org/10.1016/j.bbrc.2022.03.160.
Wei, J., Zhou, T., Hu, Z., Li, Y., Yuan, H., Zhao, K., Zhang, H., Liu, C., 2018. Effects of triclocarban on oxidative stress and innate immune response in zebrafish embryos. Chemosphere 210, 93–101. https://doi.org/10.1016/j.chemosphere.2018.06.163.
Wei, L., Qiao, P., Shi, Y., Ruan, Y., Yin, J., Wu, Q., Shao, B., 2017. Triclosan/triclocarban levels in maternal and umbilical blood samples and their association with fetal malformation. Clin. Chim. Acta 466, 133–137. https://doi.org/10.1016/j.cca.2016.12.024.
Wetts, R., Serbedzija, G.N., Fraser, S.E., 1989. Cell lineage analysis reveals multipotent precursors in the ciliary margin of the frog retina. Dev. Biol. 136, 254–263. https://doi.org/10.1016/0012-1606(89)90146-2.
Wu, Y., Beland, F.A., Fang, J.-L., 2016a. Effect of triclosan, triclocarban, 2,2′,4,4′-tetrabromodiphenyl ether, and bisphenol A on the iodide uptake, thyroid peroxidase activity, and expression of genes involved in thyroid hormone synthesis. Toxicol. Vitro 32, 310–319. https://doi.org/10.1016/j.tiv.2016.01.014.
Wu, Y., Beland, F.A., Fang, J.-L., 2016b. Effect of triclosan, triclocarban, 2,2',4,4'-tetrabromodiphenyl ether, and bisphenol A on the iodide uptake, thyroid peroxidase activity, and expression of genes involved in thyroid hormone synthesis. Toxicol. Vitro 32, 310–319. https://doi.org/10.1016/j.tiv.2016.01.014.
Zenobio, J.E., Sanchez, B.C., Archuleta, L.C., Sepulveda, M.S., 2014. Effects of triclocarban, N,N-diethyl-meta-toluamide, and a mixture of pharmaceuticals and personal care products on fathead minnows (Pimephales promelas). Environ. Toxicol. Chem. 33, 910–919. https://doi.org/10.1002/etc.2511.